DEVELOPMENT AND ASSESSMENT OF LANDSLIDE SUSCEPTIBILITY IN THE PROVINCE OF CHEFCHAOUEN, NORTH-WEST MOROCCO, USING REMOTE SENSING AND GIS: A WEIGHTED OVERLAY ANALYSIS APPROACH

Lahcen DAHMANI 1*0, Said LAARIBYA10, Hafida NAIM 2, Turgay DINDAROGLU 300

DOI: 10.21163/GT_2025.202.01

ABSTRACT

This study maps landslide susceptibility in the Chefchaouen region of northwestern Morocco using remote sensing and Geographic Information Systems (GIS) with a weighted overlay analysis approach. Key environmental factors considered include slope, aspect, elevation, vegetation cover, and soil characteristics. The results show a Kappa coefficient of 0.72, indicating substantial agreement between observed and expected accuracies. The user's and producer's accuracy for low susceptibility areas is 75%, for medium susceptibility areas is 85%, and for high susceptibility areas is 80%. These findings indicate a good match between the model's predictions and actual field conditions. Validation of the Landslide Susceptibility Zoning (LSZ) map revealed that most high-risk areas are located on steep slopes in the northern and western regions of Chefchaouen. Nine major landslide-prone zones were identified, providing crucial information for stakeholders to formulate effective mitigation measures. Despite several limitations, such as the temporal scope of data and the resolution of satellite imagery, this research offers significant insights into landslide risk management in the Chefchaouen region. Future perspectives include integrating long-term climate change scenarios and improving methodology to better capture local geological complexity. This study emphasizes the importance of sustainable land and vegetation management practices to reduce landslide risks.

Key-words: Landslide Susceptibility Assessment, Remote Sensing Analysis, LULC, Chefchaouen, Weighted Overlay Analysis.

1. INTRODUCTION

Landslides, considered ordinary natural disasters, pose a threat to human life. Various factors, such as slope, altitude, precipitation, and more, can influence landslide incidence (Marín-Rodríguez et al. 2024). In our study region, satellite imagery is employed to recognize and assess the impact of these elements on landslide occurrences (Ali et al., 2023; Arumugam et al., 2023). The Rif mountains are located in the north-western part of Morocco. Chefchaouen considered a captivating geographical landscape marked by intricate topographical features (**Fig. 1**) and a variety of climatic conditions (Cheddadi et al. 2015; Muller et al. 2015).

Chefchaouen's susceptibility to various geomorphological processes, especially landslides, underscores the necessity of unraveling intricate interactions shaped by human activities (Bukhari et

¹ Faculty of Humanities and Social Sciences, Laboratory of Territories, Environment, and Development, Ibn Tofail University, Kenitra, Morocco. * Corresponding author (LD) lahcen.dahmani@uit.ac.ma; (SL) said.laaribya1@uit.ac.ma.

² Faculty of Humanities and Social Sciences, Geosciences Laboratory, Ibn Tofail University, Kenitra, Morocco. (HN) Naim.hafida@uit.ac.ma

³ Faculty of Forestry, Department of Forest Engineering, Karadeniz Technical University, Trabzon, Türkiye. (TD) turgay.dindaroglu@ktu.edu.tr

al. 2023; Obda et al. 2024). Urbanization, agriculture, and deforestation affect land use, vegetation, and slope stability.

Geospatial data and GIS techniques were used to map and assess landslide susceptibility in Chefchaouen. (Laaribya et al. 2021; Arumugam et al. 2023). These technologies serve as indispensable tools, providing a comprehensive view of the spatial allocation and intensity of landslides.

The selection of Chefchaouen as the focal point of this study was grounded in its susceptibility to natural disasters, particularly landslides. Factors such as local slope, orientation, curvature, lithology, geology, and drainage characteristics accentuate the heightened risk of landslides in this region (Chebli et al. 2021; Ali et al. 2023). Moreover, Chefchaouen's complex topography and climatic variability present a distinctive challenging terrain, necessitating comprehensive research on landslides (El Amiri et al. 2024; Ghallab et al. 2024).

As natural disasters, including landslides, continue to pose imminent threats to lives, economic assets, and environmental sustainability (Sharma et al. 2024; Tayebi et al. 2024), this study aims to contribute invaluable insights into effective disaster preparedness, mitigation, and sustainable land management in Chefchaouen.

This research aims to investigate the relationship between physiographic characteristics and landslide vulnerability in Chefchaouen using advanced remote sensing and GIS technologies. The dual objectives are to create a detailed landslide susceptibility map and assess how integrating remote sensing and GIS parameters can refine vulnerability cartography. The results will help identify highrisk areas and develop targeted conservation and restoration strategies.

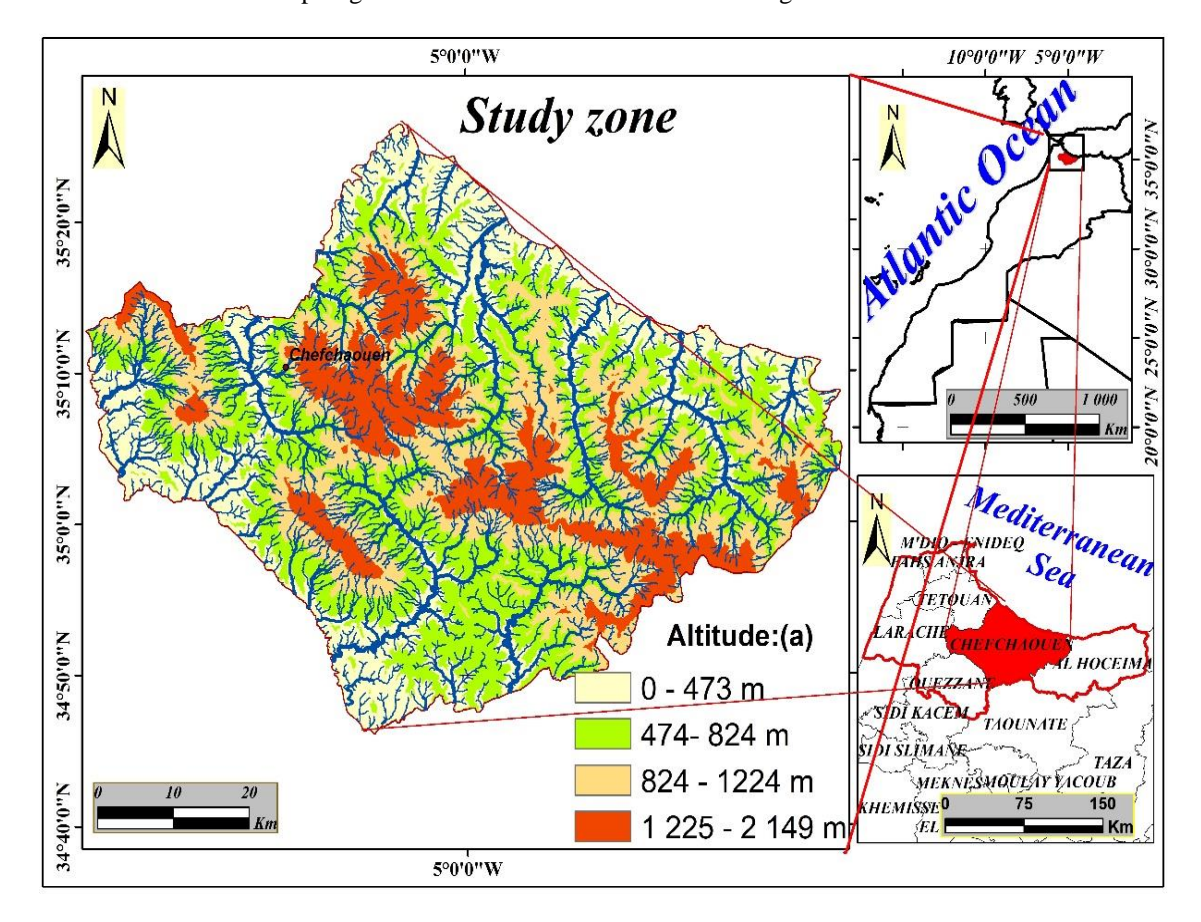


Fig. 1. Provides a visual representation of the study area, highlighting its geographical features and spatial extent.

2. STUDY AREA

Unsupervised classification using the ISODATA algorithm identified LULC categories like settlements, forests, agriculture, and water bodies in 2022. The results will be validated through field visits (Fig. 2). Thus, we have measured flows of different nature. Table 1 shows an example of indicators of material and energy flows of urban environment for subsystem of city economy, which includes 16 indicators.

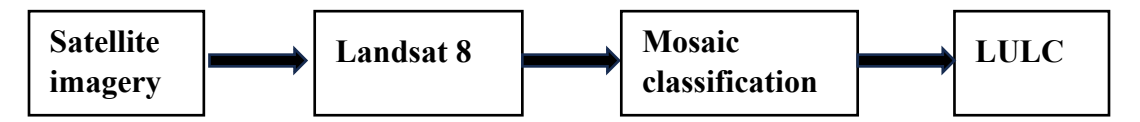


Fig. 2. Visually represents the unsupervised classification process, outlining the steps involved in identifying changes in LULC patterns as proposed by Lu et al. (2019) and Verma and Jana (2019).

COLLECTION AND ANALYSIS OF DATA

3.1. Lithology

Chefchaouen, situated in the Rif Mountains of Morocco, has a geological landscape primarily composed of sedimentary rocks and flysch formations. The combination of this geological makeup, rugged terrain, rock weathering, clay layers, tectonic activity, and heavy rainfall contribute to the region's susceptibility to landslides. These factors lead to slope instability, posing significant risks to infrastructure and the local population (Chalouan et al. 2008; Morino, Coratza & Soldati 2022) (Fig. 3a).

3.2. Precipitation

The northern and western parts of Chefchaouen have altitudes of over 825 meters and are considered the areas most affected by landslides. Rainfall in the Chefchaouen region generally increases from south to north (Fig. 3b). This rainfall distribution makes the northern and slightly western parts of the region more prone to landslides. The rainy season extends from November to March, when it rains the most is most intense. Heavy rainfall during this period increases water pressure on the ground, weakening the slope and increasing the danger of landslides. As a result, regions with a higher risk are more prone to landslides. Rainfall data show that the Chefchaouen region in northern Morocco receives its heaviest rainfall in December January, February, and March. This period corresponds to the main rainy season within a specified locality (El Kharim et al., 2021a; Salhi et al., 2019).

3.3. Lineament density

The geologically complex Chefchaouen region is characterized by a dense network of linear features known as lineaments, which play a significant role in influencing landslides (Ramli et al. 2010a; Obda et al. 2024). These features create weaknesses in the rock formation, enhance water infiltration and erosion, and can potentially act as slip planes. Moreover, lineaments serve as pathways for groundwater flow, which contributes to soil saturation (Wu et al. 2021). Therefore, it is essential to map and analyze these features to effectively assess risk areas and guide geological hazard management in Chefchaouen's mountainous terrain (El Kharim et al., 2021c; Ramli et al., 2010b; Sadiq et al., 2022b) (**Fig. 3c**).

3.4. Land Use and Land Cover (LULC)

Landslides are generally influenced by land use and land cover (LULC) (Dahmani et al., 2024; Laaribya et al., 2024). the map depicting LULC in the study area, shown in figure 3d, classifies the whole area into seven distinct categories using unsupervised classification. These are urban areas (12%), dense forests (19%), plantations (14%), agriculture (21%), mixed residential and agricultural areas (11%), other (17%), and water bodies (7%) (**Fig. 4**).

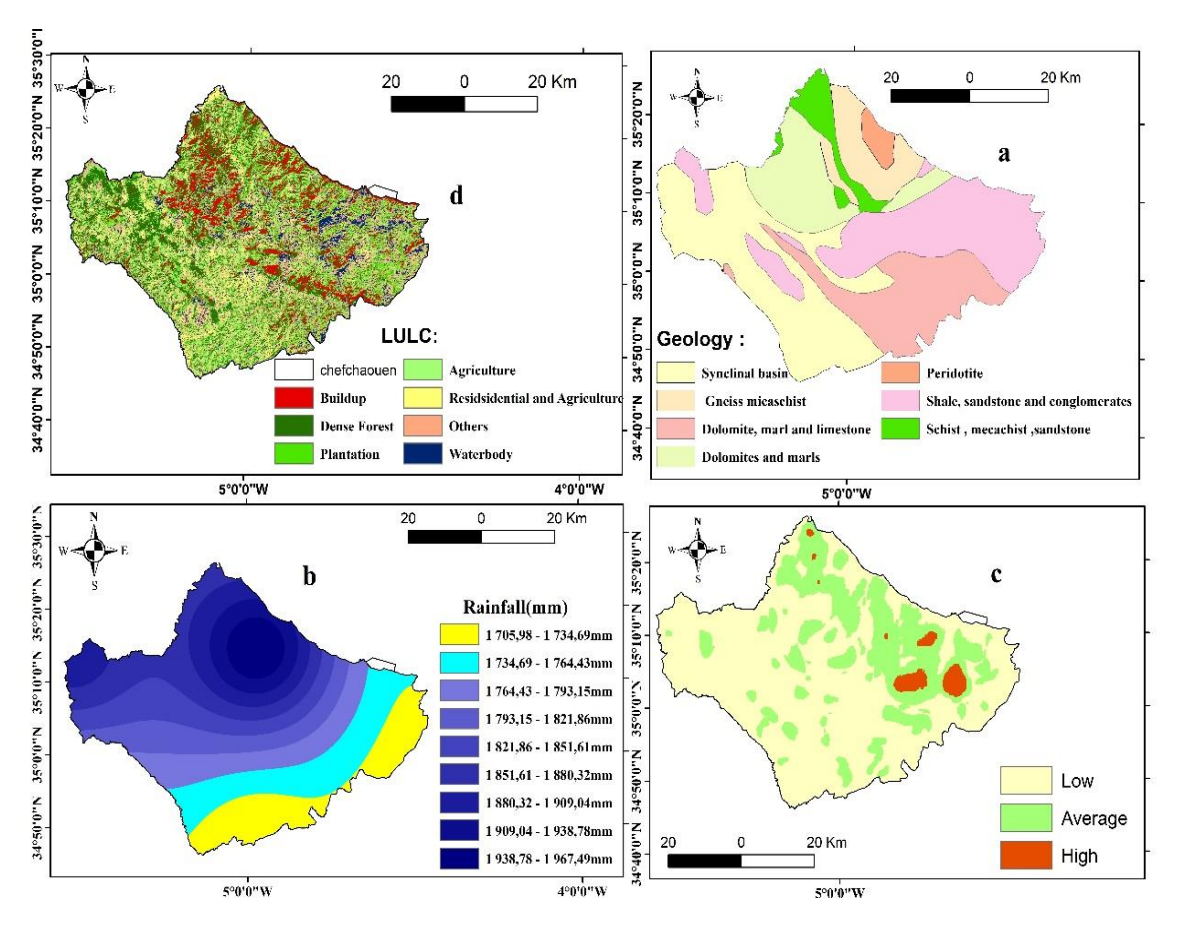


Fig. 3. a) Lithology Map of Chefchaouen, Morocco (Mastere, Van Vliet-Lanoë & Brahim 2013; Obda et al. 2024) (*Modified and Simplified*); b) illustrates the rainfall map of the Chefchaouen study area, depicting the spatial distribution of precipitation and its potential impact on landslide susceptibility; c) dense network of linear features; d) LULC.

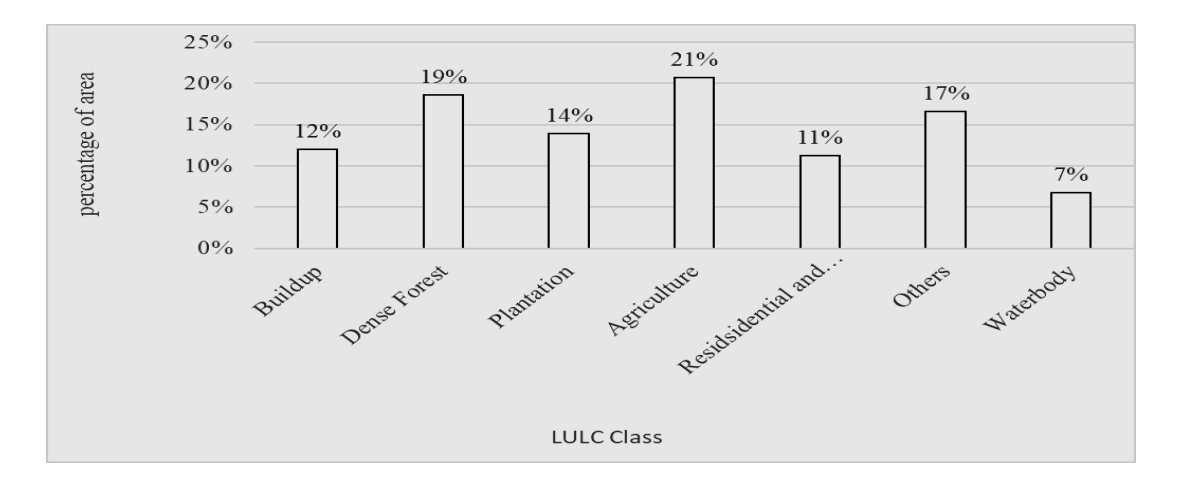


Fig. 4. Exploring the graph showing the percentage of land use and occupation by zone in the Chefchaouen study area, providing insights into spatial variations in human-environment interactions.

3.5. Elevation

Large-scale landslides are crucial factors influencing landslides (El Jazouli, Barakat & Khellouk 2019; Wu et al. 2023). An elevation model with a precision of 30 m was created using ArcGIS technology. Figure 1 a depicts the geographical setting of the research region on the elevation map is created using DEM (digital terrain model) and exists classified into four types: 0-473 m, 474-824 m, 825-1224 m, and 1225-2149 m. The altitude of Chefchaouen and its rainfall distribution highlight the vulnerability of the northern and western regions, emphasizing the interplay between high rainfall, altitude, and landslide risk. The distribution of altitudes in the Chefchaouen region is shown in **figure** 5-a1.

3.6. Slope

The incline, which represents the steepness of a surface, is generally acknowledged that more inclined slopes are prone to landslides because of gravitational factors. (Maleika 2020; Zhao, Liu & Xu 2021). In this study, slope data were extensively utilized to create a landslide vulnerability map. The incline map, generated from Digital Terrain Model (DTM) data, is divided into four categories: 0-14, 15-34, 35-54, and 55-75 degrees (**Fig. 5b**). As the slope increases, the peak stress at the base of the slope inclines, steeper slopes become more likely to experience distortion and collapse According to the classification, the study area, particularly the northern regions, features steep slopes ranging from 54 to 74 degrees. Notably, the city of Chefchaouen and the northern and northeast regions exhibit slopes steeper than 35° (El Kharim et al., 2021a; Jin et al., 2022). Landslides within the study region are concentrated on slopes in mountainous areas exceeding 10°, with the 0 to 14° slope areas experiencing no landslide events (Dahmani et al., 2024), map and graphical data in the figure 5-b1.

3.7. Aspect

The terrain slope is generally measured in degrees and varies from 0 to 360 degrees. This is an important variable in landslide research, because it influences solar radiation, wind, precipitation, and instability conditions (Auflič et al. 2023). According to Somnath and colleagues (2019), the ground experiences varying amounts of solar radiation depending on its slope, which affects vegetation cover, surface evaporation and the landslides that occur

In figure 5c, an aspect maps the segmentation derived from the DEM data for the region under analysis is illustrated, categorized into segments oriented towards the northeast, southeast, southwest, and northwest directions. This division is attributed to the influence of solar radiation, landslides occur more frequently in the west, northwest, and southwest than in the east, according to the data from the aspect map and figure 5-c1, North-East (N-E): 25%, East-South (E-S): 23%, Southwest (S-W): 26%, West-North (W-N): 25%.

Table 1. Slope classes and their percentage distribution in the study area.

Slope (degree)	Percentage distribution	Where			
0 - 14	38%	predominantly in the south and west.			
15 – 34	55%	mainly in the southwest, west, and east			
35 - 54	6%	primarily in the north, northeast, and southeast.			
55 - 75	1%	mainly in the north near the city of Chefchaouen			

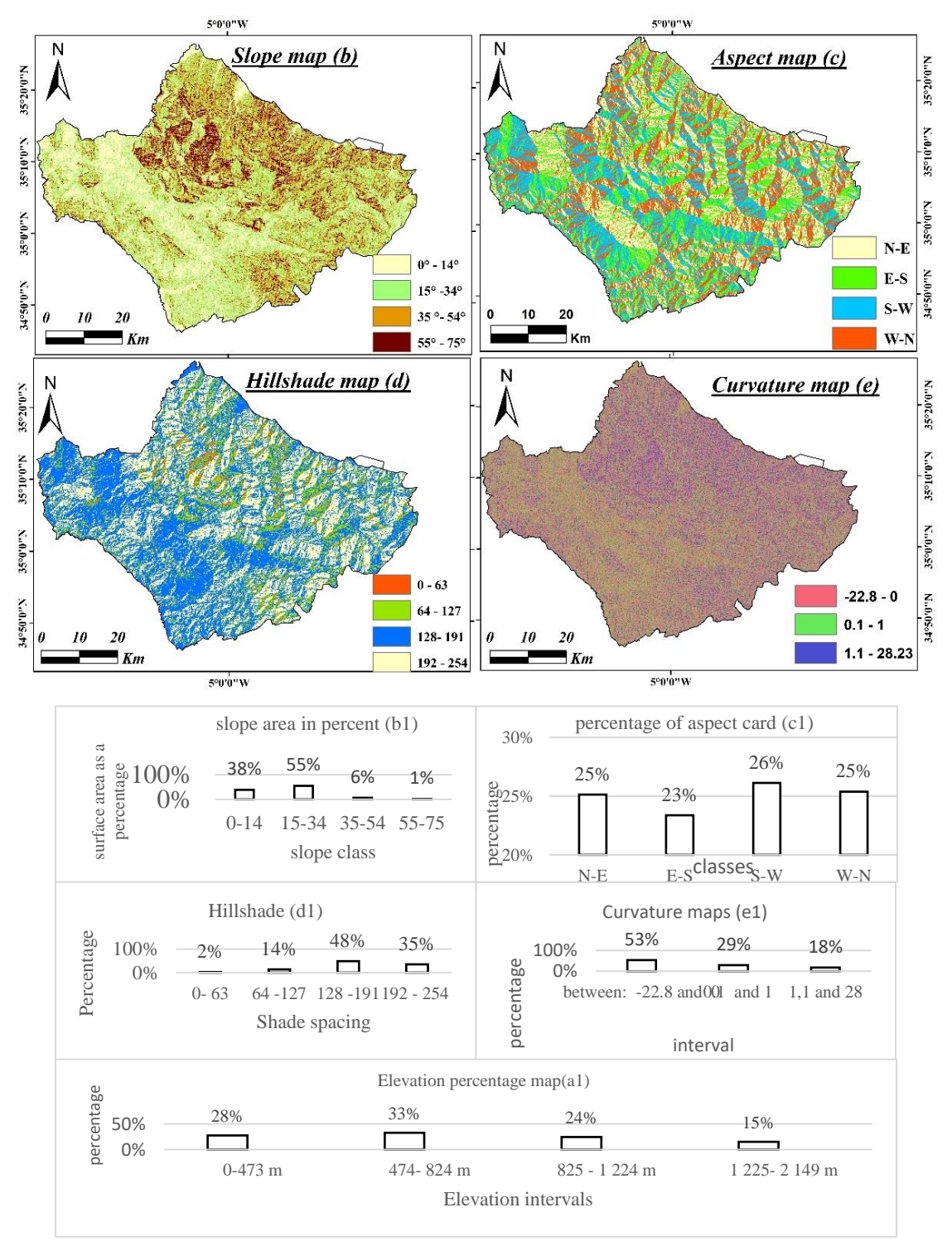


Fig. 5. Percentage distribution of factors: slope map (b); aspect map (c); hillslope map (d); curvature map (c); slope area in percentage (b1); percentage of aspect card (c1); hillshade percentage (d1); cuvature map percentage (e1); elevation percentage (a1).

3.8. Hillshade

Chefchaouen shadow map provides information about solar radiation on different mountain slopes, the intensity of shadows and changes in solar radiation in the region. It can also be used to assess the effects of shading on phenomena such as sunlight availability, soil temperature, and plant growth. (Fig. 5). A more detailed analysis of the shade map of the Chefchaouen Mountains requires, in addition to the map itself, information on the method of map creation, the shade parameters, and the specific objective of the study (**Fig. 5d**) (Qi et al. 2021). **Figure 5-d1** are shown the distribution in percentage of each class.

3.9. Curvature

The orientation of slopes concerning topographic slopes is typically measured in north latitude and ranges from 0 degrees to 360 degrees. This factor is pivotal in landslide occurrence research as it influences slope radiation, wind direction, precipitation, and failure conditions (Pacheco Quevedo et al. 2023) impact of solar radiation on the ground varies with slope, affecting vegetation density, soil erosion the process of evaporation, leading to landslides. Solar slopes retain less water due to the process of evaporation by solar radiation, as explored by various researchers (Arumugam et al. 2023). Consequently, plants located on sunlit slopes, including grasses, survive drought and radiation better. For the specific case of Chefchaouen province in northern Morocco, this study shows that the slope orientation map obtained from DEM data comprises segments northeast, southeast, southwest, and northeast. to the west (**Fig. 5e**) (Liu et al. 2021).

Under the influence of solar radiation, landslides occur more often in the west, northwest, and southwest directions than in the probable directions, and a smaller curvature indicates an effect (Jerez et al. 2021; Jin et al. 2022). Analysis of the curvature map reveals significant variations that could influence landslide susceptibility. Figure 5e and figure 5-e1 show the distribution of curvature in the study area.

METHODS

4.1. Inverse Distance Weighting Approach (IDW)

The IDW method performs spatial interpolation by assigning values to points based on their distance, with closer points having greater influence than distant ones. (Li et al. 2020; Maleika 2020). IDW can effectively manage evenly distributed points with a more uniform weight distribution among neighboring points because of its lower power requirement (Arumugam et al., 2023; Kinattinkara, et al., 2020). We collected DGM precipitation data from 1992 to 2022 and interpolated them using the IDW method. A precipitation map was created to display the average precipitation.

4.2. Analyzing with Weighted Overlay Analysis (WOA)

The statistical technique known as Weighted Overlay Analysis (WOA) is frequently employed to allocate weights derived from the interaction incorporating causal factors of landslides considering the occurrence frequency of landslides. This method follows an overlay principle where values are assigned according to the overlay, and this process can be easily expanded to include additional criteria. Each stratum illustrated on the thematic map receives a numerical value based on its significance across all corresponding layers. Subsequently, these weighted layers are overlaid, resulting in the creation of a comprehensive map. Landslide Hazard Zoning Map (LHZ) is produced by overlaying thematic maps using the weighted overlay method. Figure 6 depicts the comprehensive steps of the preparation procedure.

This method, known as Weighted Overlay Analysis, is a statistical approach used to merge thematic maps. It assigns weights to each map based on its significance, creating a composite map representing an aggregated risk or value. The weight assignment involves allocating weights to each map (e.g., slope, vegetation, proximity to water bodies) based on their presumed impact on the target phenomenon.

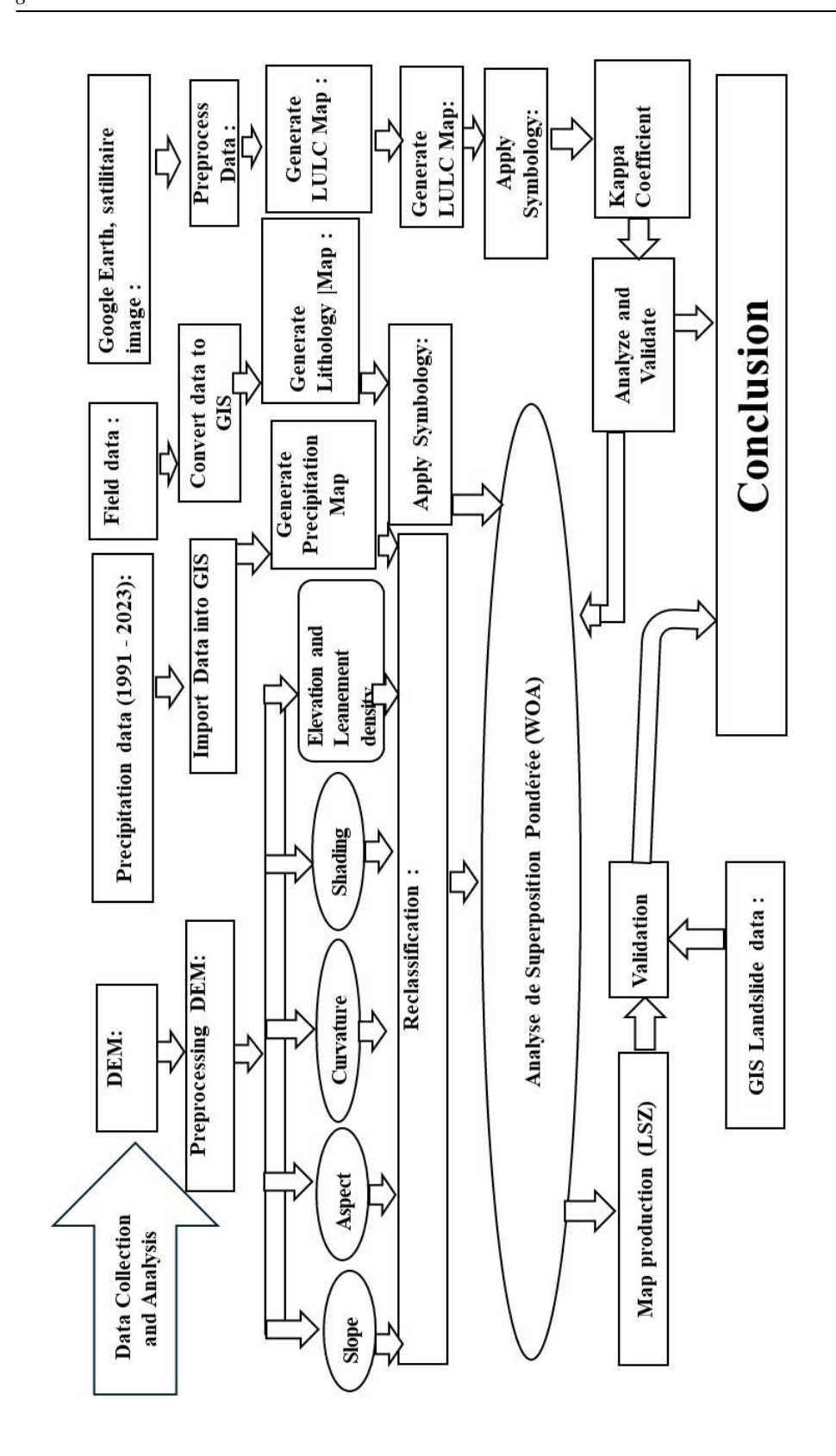


Fig. 6. Workflow for the preparation of landslide zooning map.

Numerical values are then assigned to each map based on specific characteristics, such as a higher slope receiving a higher assigned value. The weighted sum calculation involves multiplying the values of each map by their respective weights and combining the results. The calculation relationship within the WOA can be summarized by the following formula:

Composite Value =
$$(Map\ Value\ 1 \times Map\ Weight\ 1) + (Map\ Value\ 2 \times Map\ Weight\ 2) + (Map\ Value\ 3 \times Map\ Weight\ 3) + (Map\ Value\ 4 \times Map\ Weight\ 4 + ...$$
 (1)

Composite Value = $(slope\ value \times slope\ weight) + (aspect\ value \times aspect\ weight) +$

- + (elevation value \times elevation weight) + (lithology value \times lithology weight)
- + (land use value \times land use weight) + (precipitation value \times precipitation weight) +
- + (distance to faults value × distance to faults weight)

Higher values on the composite map indicate a higher level of the studied phenomenon, such as an increased risk of landslides. In summary, WOA combines information from diverse maps, considering their relative importance, to generate a synthetic map highlighting areas of elevated risk. **Figure 6** illustrates the workflow for the preparation of landslide zoning maps.

RESULTS AND DISCUSSION

Different types of factors were assigned ordered weights, with larger weights signifying greater impacts on the incidence of landslides (Basharat et al., 2016). The Landslide Susceptibility Zoning (LSZ) map for the study area was constructed, factoring in key elements such as slope, elevation, rainfall and land use and land cover (Fig. 7).

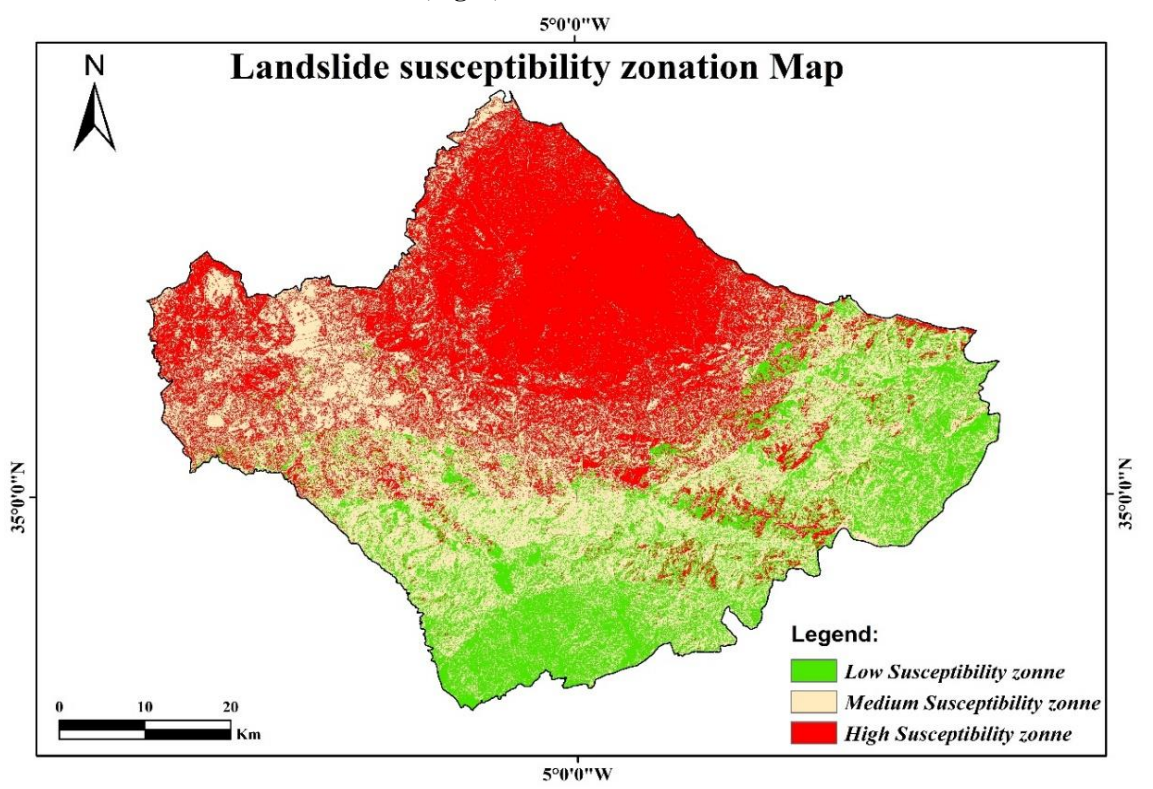


Fig. 7. Illustrates the landslide susceptibility zoning map of the Chefchaouen study area, highlighting different zones based on their susceptibility to landslides.

Using a weighted analysis technique with ArcGIS tools, the LSZ map was created by defining an index map layer for these features. **Table 2** shows the percentage of indicating landslide susceptibility as a function of land use and land cover (LULC). The analysis can be summarized as follows: in areas with low landslide susceptibility (LSZ), dense forests and plantations were the highest proportions (6% and 5%, respectively). Agricultural, mixed, other and water areas have a proportion of 2%. For average landslide susceptibility (LSZ), agricultural and other zones had the highest proportions (9% each), followed by dense forests (8%) and mixed zones (6%). Built-up areas, plantations and water areas have a lower proportion (2%, 5% and 2% respectively). In terms of high landslide susceptibility (LSZ), built-up and agricultural areas represent the highest proportion (10% each), followed by other areas (6%) and dense forests (5%). Plantations, mixed zones and water areas have a lower proportion (4%, 3% and 1% respectively), suggesting that built-up agricultural areas are more likely to be affected by landslides, while water areas are the least likely (**Table 2**).

Table 2. The distribution of LULC types according to LSZs in the Chefchaouen study area, providing insights into the spatial variation of land cover within different susceptibility zones.

LSZ	LULC								
	Buildup	Dense	Plantation	Agriculture	Mixed	Others	Water		
		Forest							
Low	0%	6%	5%	2%	2%	2%	4%		
Medium	2%	8%	5%	9%	6%	9%	2%		
High	10%	5%	4%	10%	3%	6%	1%		

5.1. Accuracy Assessment of Geological Factors Influencing Landslides

The evaluation of precision in land use was conducted using 140 control points (**Table 3**).

Table 3
The accuracy assessment results of land use classification for different land use categories, providing insights into the reliability of classification results for each category.

Land use	Buildup	Dense Forest	Plantation	Agriculture	Mixed	Others	Water	Total	User's accuracy (%)		
Buildup	15	1	1	1	1	1	0	20	0,75		
Dense Forest	1	16	1	0	1	1	0	20	0,80		
Plantation	0	1	16	1	1	1	0	20	0,80		
Agriculture	0	0	1	14	0	5	0	20	0,70		
Mixed	2	0	0	1	15	2	0	20	0,75		
Others	2	2	1	3	2	10	0	20	0,50		
Water	0	0	0	0	0	0	20	20	1,00		
Total	20	20	20	20	20	20	20	140	0,76		
Producer's accuracy (%)	0,75	0,80	0,80	0,70	0,75	0,50	1,00		0,76		
Kappa							0,72				

The Kappa coefficient of 0.72 indicates substantial agreement between observed and expected accuracies. The accuracy assessment of landslide susceptibility mapping (LSZ) was carried out with 60 control points. The results show a user and producer accuracy of 75% for low susceptibility areas, 85% for medium susceptibility areas, and 80% for high susceptibility areas. These accuracy measures provide an evaluation of how well the LSZ map corresponds to the actual distribution of landslide susceptibility categories, demonstrating satisfactory agreement between observed and expected accuracy (**Table 4**).

Table 4.

Agreement between observed and expected accuracy for different land use categories.

Land Use Type	Built-up	Dense Forest	Plantations	Agricultural	Mixed	Other	Water
	Areas	Areas	1 iantations	Areas	Areas	Areas	Areas
User' Accuracy	75%	80%	80%	70%	75%	50%	100%
Producer's Accuracy	75%	80%	80%	70%	75%	50%	100%

5.2. Validation of the Landslide Susceptibility Zonation Map

To Field validation at five sites in Chefchaouen confirmed the LSZ map's accuracy (**Fig. 8**). Observations matched predicted susceptibility levels, with minor discrepancies analyzed. This process improved the map's reliability and future mapping techniques.



Fig. 8. Landslides in northern Chefchaouen: recent events and local testimonies (20/07/2024 - 01/08/2024).

5.3. Limitation of The Study

Our landslide susceptibility study in Chefchaouen faces limitations, including restricted temporal data, moderate image resolution, and limited validation sites. Rapid urbanization, climate change scenarios, and geological complexity are not fully captured. The lack of detailed historical landslide data also affects model validation, requiring careful result interpretation and future research.

6. CONCLUSIONS

The results of the association between the Land Use and Land Cover (LULC) maps and landslides reveal crucial information about the susceptibility of different areas.

In the context of the study focused on severe natural disasters, especially landslides, it revealed distinctive geological and climatic conditions leading to frequent occurrences in the northwest region. Factors such as slope, orientation, curvature, hillshade and height are considered to minimize slope stability. This study identified high-risk landslide zones in the north and west regions, mainly on steep slopes. Nine major landslide-prone zones were identified, assisting stakeholders in formulating effective mitigation measures based on Landslide Susceptibility Zone (LSZ) maps.

This study emphasized the importance of comprehensive information from risk areas, providing insights into current and potential landslides. This information proves valuable in mitigating construction challenges related to landslides, and benefits the public, engineers, and urban planners. Effective modeling and implementation of mitigation measures are crucial to addressing landslide risks in the northwest region of Morocco.

According to maps and field visits, deforestation in the northwest and the presence of a water body in the north, due to heavy precipitation from the northern regions as opposed to the southern ones, play a part in shaping the present landscape. This research identified high-risk landslide zones in the north and west regions, mainly on steep slopes. Nine major landslide-prone zones are identified, assisting stakeholders in formulating effective mitigation measures based on Landslide Susceptibility Zone (LSZ) map.

REFERENCES

- Ali, S.A., Mohajane, M., Parvin, F., Varasano, A., Hitouri, S., Łupikasza, E., Pham, Q.B., 2023. Mass movement susceptibility prediction and infrastructural risk assessment (IRA) using GIS-based Meta classification algorithms. Appl Soft Comput 145, 110591. https://doi.org/10.1016/j.asoc.2023.110591
- Arumugam, T., Kinattinkara, S., Velusamy, S., Shanmugamoorthy, M., Murugan, S., 2023. GIS based landslide susceptibility mapping and assessment using weighted overlay method in Wayanad: A part of Western Ghats, Kerala. Urban Clim 49, 101508. https://doi.org/10.1016/j.uclim.2023.101508
- Auflič, M.J., Herrera, G., Mateos, R.M., Poyiadji, E., Quental, L., Severine, B., Peternel, T., Podolszki, L., Calcaterra, S., Kociu, A., Warmuz, B., Jelének, J., Hadjicharalambous, K., Becher, G.P., Dashwood, C., Ondrus, P., Minkevičius, V., Todorović, S., Møller, J.J., Marturia, J., 2023. Landslide monitoring techniques in the Geological Surveys of Europe. Landslides 20, 951–965. https://doi.org/10.1007/s10346-022-02007-1
- Bukhari, M.H., da Silva, P.F., Pilz, J., Istanbulluoglu, E., Görüm, T., Lee, J., Karamehic-Muratovic, A., Urmi, T., Soltani, A., Wilopo, W., Qureshi, J.A., Zekan, S., Koonisetty, K.S., Sheishenaly, U., Khan, L., Espinoza, J., Mendoza, E.P., Haque, U., 2023. Community perceptions of landslide risk and susceptibility: a multi-country study. Landslides 20, 1321–1334. https://doi.org/10.1007/S10346-023-02027-5/METRICS
- Chalouan, A., Michard, A., Kadiri, K. El, Negro, F., Frizon de Lamotte, D., Soto, J.I., Saddiqi, O., 2008. The Rif Belt. Lecture Notes in Earth Sciences 116, 203–302. https://doi.org/10.1007/978-3-540-77076-3_5
- Chebli, Y., Otmani, E., National, I., Agronomique, D.R., Mohamed, B., Abdellah, B., 2021. du Rif occidental (Chefchaouen) 180–200.
- Cheddadi, R., Nourelbait, M., Bouaissa, O., Tabel, J., Rhoujjati, A., López-Sáez, J.A., Alba-Sánchez, F., Khater, C., Ballouche, A., Dezileau, L., Lamb, H., 2015. A History of Human Impact on Moroccan Mountain Landscapes. African Archaeological Review 32, 233–248. https://doi.org/10.1007/S10437-015-9186-7/METRICS
- Dahmani, Lahcen, Laaribya, S., Naim, H., Dindaroglu, T., 2024. Landslide hazard mapping in Chefchaouen, Morocco: AHP-GIS integration. International Journal of Environmental Studies. https://doi.org/10.1080/00207233.2024.2412483

- El Amiri, B., Azmi, R., Laaribya, S., Dani, B., Sibaoueih, M., Omar, B., 2024. The Drought Resilience of Vast Livestock Reared in Agropastoral Versus Sylvo-Agro-Pastoral Systems in Morocco 99–110. https://doi.org/10.1007/978-3-031-59603-2_7
- El Jazouli, A., Barakat, A., Khellouk, R., 2019. GIS-multicriteria evaluation using AHP for landslide susceptibility mapping in Oum Er Rbia high basin (Morocco). Geoenvironmental Disasters 6. https://doi.org/10.1186/s40677-019-0119-7
- El Kharim, Y., Bounab, A., Ilias, O., Hilali, F., Ahniche, M., 2021a. Landslides in the urban and suburban perimeter of Chefchaouen (Rif, Northern Morocco): inventory and case study. Natural Hazards 107, 355–373. https://doi.org/10.1007/S11069-021-04586-Z/METRICS
- El Kharim, Y., Bounab, A., Ilias, O., Hilali, F., Ahniche, M., 2021b. Landslides in the urban and suburban perimeter of Chefchaouen (Rif, Northern Morocco): inventory and case study. Natural Hazards 107, 355–373. https://doi.org/10.1007/S11069-021-04586-Z/METRICS
- Ghallab, A., Boubekraoui, H., Laaribya, S., Ben-Said, M., 2024. Potential natural vegetation pattern based on major tree distribution modeling in the western Rif of Morocco. IForest 17, 405. https://doi.org/10.3832/IFOR4602-017
- Jerez, S., Palacios-Peña, L., Gutiérrez, C., Jiménez-Guerrero, P., María López-Romero, J., Pravia-Sarabia, E., Montávez, J.P., 2021. Sensitivity of surface solar radiation to aerosol-radiation and aerosol-cloud interactions over Europe in WRFv3.6.1 climatic runs with fully interactive aerosols. Geosci Model Dev 14, 1533–1551. https://doi.org/10.5194/gmd-14-1533-2021
- Jin, H., Wang, S., Yan, P., Qiao, L., Sun, L., Zhang, L., 2022. Spatial and temporal characteristics of surface solar radiation in China and its influencing factors. Front Environ Sci 10, 1–15. https://doi.org/10.3389/fenvs.2022.916748
- Kinattinkara, S., Arumugam, T., Poongodi, K.S., 2020. Surveillance of groundwater quality of selected rural and industrial areas of Coimbatore: A GIS Approach. IOP Conf Ser Mater Sci Eng 955. https://doi.org/10.1088/1757-899X/955/1/012083
- Laaribya, S., Alaoui, A., Ayan, S., Benabou, A., Labbaci, A., Ouhaddou, H., Bijou, M., 2021. Prediction by maximum entropy of potential habitat of the cork oak (Quercus suber L.) in Maamora Forest, Morocco. Forestist 71, 63–69. https://doi.org/10.5152/forestist.2021.20059
- Laaribya, S., Alaoui, A., Ayan, S., Dindaroglu, T., 2023. Changes in the Potential Distribution of Atlas Cedar in Morocco in the Twenty-First Century According to the Emission Scenarios of RCP 4,5 and RCP 8,5. Forestist. https://doi.org/10.5152/forestist.2023.0004
- Li, Z., Zhang, X., Zhu, R., Zhang, Z., Weng, Z., 2020. Integrating data-to-data correlation into inverse distance weighting. Comput Geosci 24, 203–216. https://doi.org/10.1007/s10596-019-09913-9
- Liu, C., Huang, Y., Wu, F., Liu, W., Ning, Y., Huang, Z., Tang, S., Liang, Y., 2021. Plant adaptability in karst regions. J Plant Res 134, 889–906. https://doi.org/10.1007/s10265-021-01330-3
- Maleika, W., 2020. Inverse distance weighting method optimization in the process of digital terrain model creation based on data collected from a multibeam echosounder. Applied Geomatics 12, 397–407. https://doi.org/10.1007/s12518-020-00307-6
- Marín-Rodríguez, N.J., Vega, J., Zanabria, O.B., González-Ruiz, J.D., Botero, S., 2024. Towards an understanding of landslide risk assessment and its economic losses: a scientometric analysis. Landslides 1–17. https://doi.org/10.1007/S10346-024-02272-2/FIGURES/12
- Mastere, M., Van Vliet-Lanoë, B., Brahim, L.A., 2013. Cartographie de l'occupation des sols en relation avec les mouvements gravitaires et le ravinement dans le Rif nord-occidental (Maroc). http://journals.openedition.org/geomorphologie 335–352. https://doi.org/10.4000/GEOMORPHOLOGIE.10328
- Mohamed Mastere, B.V.V.-L. et L.A.B., n.d. Cartographie de l'occupation des sols en relation avec les mouvements gravitaires et le ravinement dans le Rif nord-occidental (Maroc).
- Morino, C., Coratza, P., Soldati, M., 2022. Landslides, a Key Landform in the Global Geological Heritage. Front Earth Sci (Lausanne) 10, 864760. https://doi.org/10.3389/FEART.2022.864760/BIBTEX

- Muller, S.D., Rhazi, L., Andrieux, B., Bottollier-Curtet, M., Fauquette, S., Saber, E.R., Rifai, N., Daoud-Bouattour, A., 2015. Vegetation history of the western Rif mountains (NW Morocco): origin, late-Holocene dynamics and human impact. Veg Hist Archaeobot 24, 487–501. https://doi.org/10.1007/S00334-014-0504-9/METRICS
- Obda, O., El Kharim, Y., Obda, I., Ahniche, M., Sahrane, R., 2024. Landslide Susceptibility Assessment and Factors' Selection Using the GIS Matrix Method (GMM) in Chefchaouen Province (Northern Morocco). Advances in Science, Technology and Innovation 197–199. https://doi.org/10.1007/978-3-031-43218-7_46
- Pacheco Quevedo, R., Velastegui-Montoya, A., Montalván-Burbano, N., Morante-Carballo, F., Korup, O., Daleles Rennó, C., 2023. Land use and land cover as a conditioning factor in landslide susceptibility: a literature review. Landslides 20, 967–982. https://doi.org/10.1007/s10346-022-02020-4
- Qi, X., Li, Q., Jiao, Y., Tan, F., 2021. Experimental study on response law and failure process of slopes in fully weathered granites under precipitation infiltration. Environ Earth Sci 80, 685. https://doi.org/10.1007/s12665-021-09995-8
- Ramli, M.F., Yusof, N., Yusoff, M.K., Juahir, H., Shafri, H.Z.M., 2010a. Lineament mapping and its application in landslide hazard assessment: a review. Bulletin of Engineering Geology and the Environment 2009 69:2 69, 215–233. https://doi.org/10.1007/S10064-009-0255-5
- Ramli, M.F., Yusof, N., Yusoff, M.K., Juahir, H., Shafri, H.Z.M., 2010b. Lineament mapping and its application in landslide hazard assessment: a review. Bulletin of Engineering Geology and the Environment 2009 69:2 69, 215–233. https://doi.org/10.1007/S10064-009-0255-5
- RGPH, 2014a. RGPH. CHEFCHAOUEN PROVINCE. https://doi.org/http://www.hcp.ma/
- RGPH, 2014b. RGPH. CHEFCHAOUEN PROVINCE. https://doi.org/http://www.hcp.ma/
- Sadiq, S., Muhammad, U., Fuchs, M., 2022. Investigation of landslides with natural lineaments derived from integrated manual and automatic techniques applied on geospatial data. Natural Hazards 110, 2141–2162. https://doi.org/10.1007/S11069-021-05028-6/METRICS
- Salhi, A., Martin-Vide, J., Benhamrouche, A., Benabdelouahab, S., Himi, M., Benabdelouahab, T., Casas Ponsati, A., 2019. Rainfall distribution and trends of the daily precipitation concentration index in northern Morocco: a need for an adaptive environmental policy. SN Appl Sci 1, 277. https://doi.org/10.1007/s42452-019-0290-1
- Sharma, A., Sajjad, H., Roshani, Rahaman, M.H., 2024. A systematic review for assessing the impact of climate change on landslides: research gaps and directions for future research. Spatial Information Research 32, 165–185. https://doi.org/10.1007/S41324-023-00551-Z/METRICS
- Tayebi, S., Jabed, M.A., Ruano, A.L., Lee, G.O., da Silva, P.F., Ahmed, S., G, E.V.A., Dahal, R.K., Soltani, A., Imran Khan, M., Rahman, M.A., Islam, M.A., Haque, U., 2024. Stakeholder perspectives on landslide triggers and impacts in five countries. Landslides 1–11. https://doi.org/10.1007/S10346-024-02270-4/TABLES/3
- Wu, J., Zhang, Ya, Yang, L., Zhang, Yongxian, Lei, J., Zhi, M., Ma, G., 2023. Identifying the essential influencing factors of landslide susceptibility models based on hybrid-optimized machine learning with different grid resolutions: a case of Sino-Pakistani Karakorum Highway. Environmental Science and Pollution Research 30, 100675–100700. https://doi.org/10.1007/s11356-023-29234-w
- Wu, X., Meng, Z., Dang, X., Wang, J., 2021. Effects of rock fragments on the water infiltration and hydraulic soils the Mongolia, conductivity in the of desert steppes of Inner China. https://swr.agriculturejournals.cz/doi/10.17221/107/2020-SWR.html 16, 151-163. https://doi.org/10.17221/107/2020-SWR
- Zhao, Z., Liu, Z. yuan, Xu, C., 2021. Slope Unit-Based Landslide Susceptibility Mapping Using Certainty Factor, Support Vector Machine, Random Forest, CF-SVM and CF-RF Models. Front Earth Sci (Lausanne) 9, 1–16. https://doi.org/10.3389/feart.2021.589630